

## Structures under cyclic loading

G. INGLEBERT, J. FRELAT and J. M. PROIX (PALAISEAU)

THE PRINCIPLE of the straightforward method proposed by J. Zarka and al. is recalled. This approach is compared to experiments for studying shot-peening, and to a numerical approach through a steady-state algorithm for studying the rolling problem.

Przypomniano zasadę bezpośredniej metody obliczeń zaproponowanej przez J. Zarkę z współautorami. Podejście to porównano z wynikami eksperymentów dotyczących kuleczkowania (śrutowania) oraz z podejściem numerycznym za pomocą algorytmu ustalonego dotyczącym problemu walcowania.

Припомнен принцип непосредственного метода расчетов, предложенный Я. Зарка с соавторами. Этот подход сравнен с результатами экспериментов, касающихся дробеструйной обработки, а также с численным подходом при помощи установленного алгоритма, касающегося проблемы прокатки.

### 1. Introduction

UNDER CYCLIC loadings, the knowledge of the stabilized limiting state of inelastic strains and residual stresses for a structure is currently admitted as quite important. For example, these residual stresses and inelastic strains will be key-parameters for studying fatigue and damage. A simple and straightforward method to achieve this limiting state has been proposed by J. ZARKA and al. ([1, 2, 3, 4]). This method can be used *whatever the shape* of the structure is, and gives the limiting state in *the whole structure*. A description of the material behaviour as a microstructure made of perfectly plastic and viscoplastic subelements linked together with linear elasticity is required; then only elastic calculations and local projections in a space of properly chosen transformed variables are needed.

The aim of this paper is to show the opportunity of using this method. So, after recalling the basic principles of the method, we will use it to solve the shot-peening problem. A comparison with experimental results is given. The rolling problem has been also treated with this method. To check the results in this case, we used the approach suggested by Nguyen Quoc Son for steady problems. This method could be very useful to study the evolution of the rolling band towards its limit state; thus we give a detailed description of it.

In both cases the comparison between the results obtained through the straightforward method and through other experimental or numerical methods is rather good as it will be seen.

## 2. Principle of the straightforward method

To obtain the limiting state, two conjugate effects are involved: the local behaviour of the material and the structural effects depending on the shape of the structure and the loading path.

### 2.1. Material behaviour

Let us first recall the assumptions for the local behaviour of the material. We consider the fundamental volume of material as a microstructure made of elementary elastic mechanisms linked together through a linear elastic matrix. Thus we remain in the field of the Standard Generalized Materials [5].

The local deformations of the inelastic mechanisms  $\varepsilon^{p(\alpha)}$  will be taken as internal variables;  $\sigma^{(\alpha)}$  will be the associated local stresses on the mechanisms. For the sake of simplicity, we will restrain ourselves to perfectly plastic mechanisms. To see how bounds could be derived when viscous effects occur, one can read [4].

Using the Hill–Mandel principle, the local stresses  $\sigma^{(\alpha)}$  could be expressed in the following way:

$$(2.1) \quad \sigma^{(\alpha)} = \mathbf{A}\Sigma - \mathbf{C}\varepsilon^{p(\alpha)},$$

where  $\Sigma$  is the macrostress (global) on the volume element,  $\mathbf{A}$  is the elastic localisation tensor on the inelastic mechanisms of the element,  $\varepsilon^{p(\alpha)}$  is a generalised tensor including the deformations of all the inelastic mechanisms of the element;  $\mathbf{C}$  is the kinematic hardening tensor and  $\mathbf{C}\varepsilon^{p(\alpha)}$  is opposite to the residual stresses on the elementary mechanisms at the level of the volume element.

The global total plastic strain could be written as

$$(2.2) \quad E = M\Sigma + E^p, \quad E^p = \mathbf{A}^T \varepsilon^{p(\alpha)}.$$

The evolution laws for each perfectly plastic mechanism are

$$(2.3) \quad f(\sigma^{(\alpha)}) \leq 0, \quad \dot{\varepsilon}^{p(\alpha)} = \lambda \frac{\partial f}{\partial \sigma^{(\alpha)}}, \quad \lambda \geq 0,$$

where  $f(\sigma^{(\alpha)})$  is a convex function defining the local yield surface for an elementary mechanism.

### 2.2. Structure

The quasi-static evolution of the structure could then be obtained by solving at each time  $t$  a linear elastic problem with initial strains  $E^p$  for the given periodic loading,  $F^d(t)$  body forces in the volume  $V$ ,  $T^d(t)$  surface forces on a given part  $S_F$  of the boundary of the structure, and  $U^d(t)$  given displacements on the complementary part  $S_U$  of the boundary

$$(2.4) \quad \begin{cases} \Sigma \text{ Statically Admissible with } F^d(t) \text{ in } V, T^d(t) \text{ on } S_F, \\ E = M\Sigma + E^p \text{ Kinematically Admissible with } U^d(t) \text{ on } S_U. \end{cases}$$

Let us write  $\Sigma^{el}$ ,  $E^{el}$ , the purely elastic solution of the problem (2.4) with  $E^p$  equal to zero.

Then the global residual stresses  $R$  on the volume element and the global inelastic strain tensor  $E^{ino}$  defined by

$$(2.5) \quad R = \Sigma - \Sigma^{el}, \quad E^{ino} = E - E^{el} = E - M\Sigma^{el} = MR + E^p,$$

are solutions of the homogeneous problem associated to Eq. (2.4):

$$(2.6) \quad \begin{cases} R \text{ S.A. with } 0 \text{ in } V \text{ and } 0 \text{ on } S_F, \\ E^{ino} = MR + E^p \text{ K.A. with } 0 \text{ on } S_U. \end{cases}$$

So the global residual stresses  $R$  are linearly dependent on the global plastic strain  $E^p$  and thus on the internal variables  $\varepsilon^{p(\alpha)}$  linked to  $E^p$  through the elastic localisation tensor  $A$ , Eq. (2.2).

### 2.3. Introduction of the transformed variables for the structure

Let us define  $\hat{Y}$  transformed variables for the structure as

$$(2.7) \quad \hat{Y} = C\varepsilon^{p(\alpha)} - AR = F\varepsilon^{p(\alpha)}.$$

These variables will be linear functions of the inelastic deformation of all the elementary mechanisms of the structure through  $R$ ; the linear function  $F$  integrates the structural effects (shape and loading) and the local inelastic behaviour which is characterized by  $C$  and  $A$ . If we introduce them in the expression of the local stresses (2.1) on the elementary mechanisms, we obtain

$$(2.8) \quad \sigma^{(\alpha)} = A(\Sigma(t) - R(t)) - \hat{Y} = A\Sigma^{el}(t) - \hat{Y}.$$

So these variables could be interpreted as opposite to the residual stresses on the elementary mechanisms at the level of the structure and will appear as the associated forces to the internal parameters if the free energy is written in terms of global elastic strain and internal parameters.

In the space of the transformed variables, the expression of the plastic yield criterion is

$$(2.9) \quad f(A\Sigma^{el}(t) - \hat{Y}) \leq 0.$$

As soon as the evolution of the purely elastic solution  $\Sigma^{el}(t)$  is known over a period, *the evolution of the yield surface with the loading path is completely known*: at each time  $t$  the yield surface is deduced from the initial one through a translation of vector  $A\Sigma^{el}(t)$ . Besides, this evolution for each local mechanism is independent of the others mechanisms in this space. Such an uncoupling of the elementary mechanisms would not be achieved in the internal parameters space: the link between local stresses  $\sigma^{(\alpha)}$  and internal parameters  $\varepsilon^{p(\alpha)}$  involves the whole structure Eq. (2.7).

Furthermore, as could be very quickly checked, the *way back from* the transformed variables to the classical ones, global residual stresses  $R$ , plastic strain  $E^p$ , internal parameters  $\varepsilon^{p(\alpha)}$ , can be achieved quite simply through elastic calculations for a regular kinematic hardening tensor  $C$ . It follows from the definitions (2.2), (2.5) and (2.7) which

allow to express global plastic strain in terms of global residual stresses and transformed variables.

$$(2.10) \quad E^p = A^T \varepsilon^{p(\omega)} = A^T (C^{-1}(\hat{Y} + AR)).$$

Thus the problem (2.6) can be rewritten with the transformed elasticity operator  $M'$  and apparent initial strain  $E^{p'}$

$$(2.11) \quad \begin{cases} R \text{ S.A. with } 0 \text{ in } V \text{ and } 0 \text{ on } S_F, \\ E^{in\epsilon} = M'R + E^{p'} \text{ K.A. with } 0 \text{ on } S_U, \end{cases}$$

where

$$M' = M + A^T C^{-1} A, \quad E^{p'} = A^T C^{-1} \hat{Y}.$$

The elastic resolution of the problem (2.11) and definitions (2.7) and (2.2) will give the complete inelastic state of the structure,  $R, E^p, \varepsilon^{p(\omega)}$ . By the way, this proves that the regular local kinematic hardening tensors  $C$  will give a regular structural operator  $F$ .

**2.4. Limiting state under cyclic loading**

This ability of coming back from the transformed parameters space to the classical one allows us to study the existence, nature and value of the limiting state in this space where the unilateral yield condition is well known separately for each elementary mechanism.

**2.4.1. Existence of the limiting state.** The existence of a periodic limiting state for stresses, and thus for the transformed variables  $\hat{Y}$ , is ensured by the general theorems for Standard Generalized Materials, [5]. This will induce a periodic limiting state of internal variables and plastic strain, Eq. (2.7) and Eq. (2.2), as soon as the structural operator  $F$  is regular. So we always obtain elastic or plastic shakedown except for some singular local behaviour  $C$ . In this last case, ratchetting may occur if  $F$  is singular, too, and a more detailed analysis is required.

**2.4.2. Nature of the limiting state.** The discrimination between elastic and plastic shakedown will be reduced to an elementary geometrical problem (Fig. 1). For each mechanism one has to check if all the yield surfaces centered on the local purely elastic stresses  $A \Sigma^{el}(t)$  for each time  $t$  in a period have a common part. For the Mises type criteria,

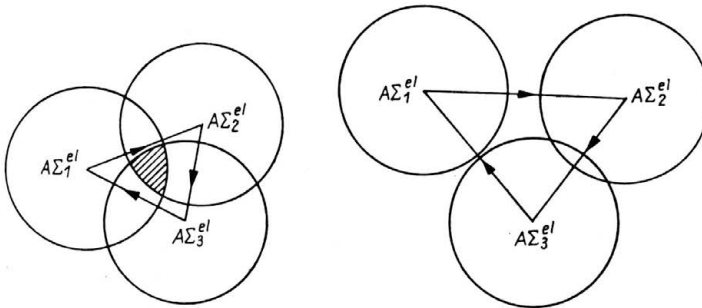


FIG. 1. Nature of the limit state.

distance between two different values of  $A \Sigma^{el}(t)$  for distinct times  $t_1$  and  $t_2$  should always be lower than twice the Mises radius. If the answer is positive for each mechanism, elastic shakedown occurs and a constant limiting state  $\hat{Y}_I$  has to be found. Otherwise a cyclic limiting state  $\hat{Y}_I(t)$  has to be estimated.

**2.4.3. Finding out the limiting state.** If the limiting state has to be known more precisely, the way to find it out can be summarised in the following:

- i. First,  $\Sigma^{el}(t)$  has to be calculated for each time  $t$  over a period.
- ii. Second, transformed variables  $\hat{Y}_I$  are locally built. The different ways to derive this local building for elastic or plastic shakedown could be found in [4]. They are based on local projection on the intersection of all the local yield surfaces over a period for elastic shakedown or on an estimate of mean value and minimum and maximum of amplitude from a local geometrical study for plastic shakedown.
- iii. Third, elastic resolution of the problem (2.11) from these  $\hat{Y}_I$  will give the global residual stresses.
- iv. Last, internal parameters  $\varepsilon^{p(\alpha)}$  and plastic strain  $E^p$  will be derived through Eqs. (2.7) and (2.2).

The method is quite convenient for numerical purposes and works rather well. It has been introduced in finite elements programs without any difficulties. Its use is much more general as will be seen in the following examples.

### 3. Applying simplified method to shot-peening

#### 3.1. Principle

Let us consider the shot-peening problem; this technique is currently used in industry: the principle is to project bullets to produce surface hardening in order to introduce "favourable residual stresses" so as to ensure a better hold against fatigue and corrosion, or to form thin sheets.

The main parameters are the shot speed and bullet size, the angle of impact, the duration of impacts and the impact surface (surface where at least one bullet has fallen).

The Almen intensity is the industrial way of control: the residual deflection of a normalised test sample is measured.

#### 3.2. Proposed model

**3.2.1. Basic hypothesis.** Let us consider a sample of material rather big with plane boundary. This sample is made of an elastoplastic material with simple linear kinematic hardening behaviour.

We expose it to a shot-peening the parameters of which are strictly defined:

The impacts of the bullets are normal to the exposed plane surface.

The bullets are spherical with a constant radius  $r$ .

The impact speed is  $V_0$  constant.

The main difficulties come from the dynamic aspect.

The needed results are mainly:

The residual stresses and plastic strains when the bombing is achieved, either in the field of elastic or plastic shakedown.

Our analysis begins when many impacts have occurred; the shot exposure is over 100%. So the elastic or plastic shakedown is reached. Then, one more bullet comes, ..., and goes ... leaving residual stresses  $R$  and plastic strain  $E^p$ .

Assuming that the exposed surface is wide enough, the equilibrium equations and the boundary conditions for the residual stresses (2.11) allow to derive that  $\mathbf{R}$  and  $E^p$  are only functions of the depth  $z$  and that the nonzero components of the residual stress tensor are

$$(12) \quad R_{xx} = R_{yy} = R(z).$$

The plastic strain tensor can easily be proved to have the following form:

$$(3.1) \quad E^p = \begin{pmatrix} E_{xx}^p = E^p(z) & 0 & 0 \\ 0 & E_{yy}^p = E^p(z) & 0 \\ 0 & 0 & E_{zz}^p = -2E^p(z) \end{pmatrix}.$$

So the "inelastic strain"  $E^{ine} = MR + E^p$  is only a function of the depth  $z$  and the transformed variables in the unloaded limiting state can be defined from only one scalar function  $\hat{\alpha}(z)$ :

$$(3.2) \quad \hat{\alpha}(z) = CE^p(z) - R(z)/3.$$

Then, only two scalar functions among  $R(z)$ ,  $E^p(z)$ ,  $\hat{\alpha}(z)$  will be sufficient to describe the solution.

Two different geometries had been considered:

a semi-infinite space  $z \geq 0$ ;

a finite plate with free edges  $-\frac{H}{2} \leq z \leq \frac{H}{2}$ .

In both cases an analytic solution can be derived from a known initial state  $E^p(z)$  or  $\hat{\alpha}(z)$ .

The last step to obtain the residual stresses in the unloaded limiting state is to build the function  $\hat{\alpha}(z)$ . Following 1.4.3, we have first to obtain the purely elastic loading path.

**3.2.2. Purely elastic loading path.** To modelize the purely elastic stresses during the contact between the spheric bullet and the sheet, we use Hertz results for the elastic contact between a sphere and a semi-infinite space. Using cylindrical coordinates with the origin

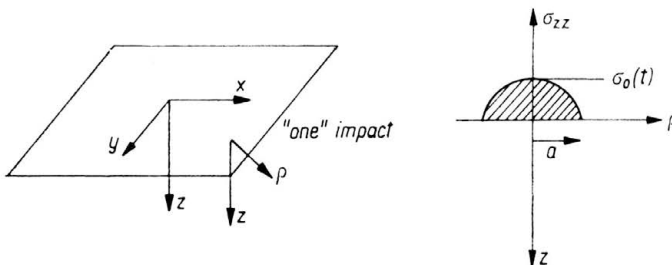


FIG. 2. Impact, coordinates, stresses distribution.

at the center of the contact area (Fig. 2), we calculate the stress field which is a function of the depth  $z$  and radial coordinate  $\rho$ . The maximum of the stress will be obtained just at the axis of the impact for a zero radial coordinate, at the impact time, say  $0^+$ . The stresses will return to zero when the sheet is completely unloaded,

$$(3.3) \quad \Sigma_1^{el}(\rho, z) = \sigma^{Hertz}(\rho, z), \quad \Sigma_2^{el}(\rho, z) = 0,$$

with, on the axis of the impact ( $\rho = 0$ ),

$$(3.4) \quad \begin{aligned} \sigma_{rr}^{Hertz} = \sigma_{\theta\theta}^{Hertz} &= \left[ (1+\nu) \left( \frac{z}{a} \text{Arctg} \frac{a}{z} - 1 \right) + \frac{1}{2} \frac{a^2}{a^2+z^2} \right] \sigma_0, \\ \sigma_{zz}^{Hertz} &= -\frac{a^2}{a^2+z^2} \sigma_0, \quad \rho = 0, \end{aligned}$$

where  $\sigma_0$  is the maximum stress on the contact area and  $a$  the radius of this area.

One particular point of the sheet will overlook a most complicated loading path with an alternance of all the possible values of  $\sigma^{Hertz}(\rho, z)$ , depending on the distance between the studied point  $(x, y)$  to the impact one, and zero values. If the scattering of the bullets is good enough, the loading path followed by the center of the yield surface will be equivalent to a symmetrical one oscillating between a zero value and the maximum value of  $\sigma^{Hertz}$  for a zero  $\rho$  situated on the  $(\hat{\alpha}_{jr} = \hat{\alpha}_{\theta\theta} = -\frac{1}{2} \hat{\alpha}_{zz})$  axis.

The involved constants  $\sigma_0$  and  $a$  are evaluated thanks to Davies' work [7] on dynamic

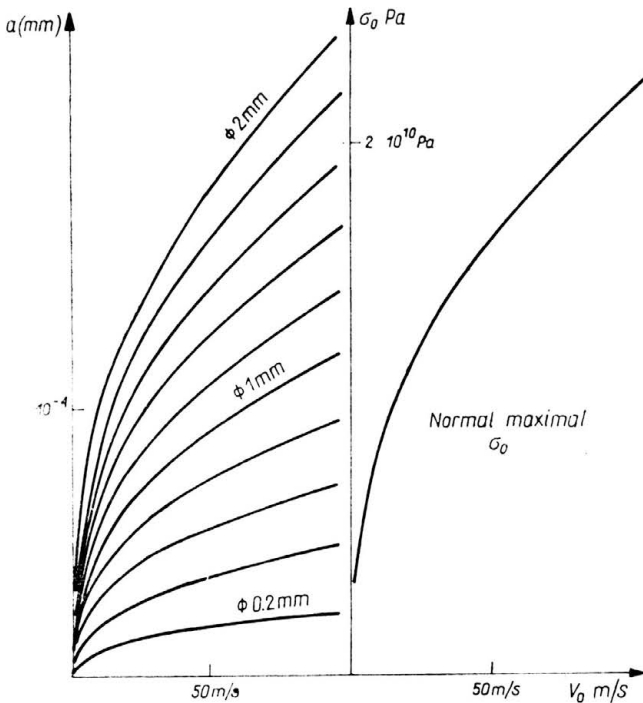


FIG. 3. Evolution of  $a$  and  $\sigma_0$  versus  $V_0$ ; ( $\phi = 2r$ ).

elastic contact between a half-space and a ball of radius  $r$ . Denoting  $V_0$  the shot speed,  $E, \nu, \rho$  the common elastic constants and mass density of the ball and the half-space, they could be written as

$$(3.5) \quad a = \left\{ \frac{5\pi}{2} \rho \frac{1-\nu^2}{E} \right\}^{1/5} r V_0^{2/5},$$

$$\sigma_0 = \frac{1}{\pi} \left\{ \frac{5\pi}{2} \rho \left( \frac{1-\nu^2}{E} \right)^4 \right\}^{1/5} V_0^{2/5}.$$

The evolution of  $a$  for various radii  $r$  and  $\sigma_0$  against  $V_0$  for a given material are plotted in Fig. 3.

**3.2.3. Local building of  $\hat{\alpha}(z)$  for each  $z$ .** For the currently used values of the shot-speed, the plastic shakedown regime is achieved. For various depths  $z$ , the local loading path  $\text{dev}(\Sigma^{el}(t))$  and yield surface could be schematically described by Fig. 1. From Fig. 4. a to Fig. 4. c, the distance between the extreme loading values decrease as the depth  $z$  increases.

When a void intersection is observed, Fig. 4. a, the symmetry conditions will give  $\hat{\alpha}$  in the unloaded state as the point of the yield surface closest to the maximal loaded state.

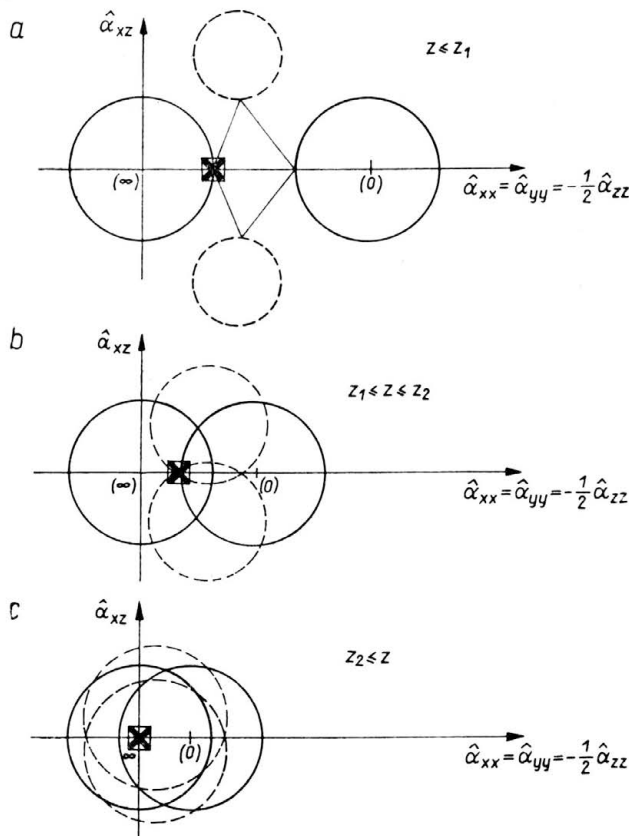


FIG. 4. Local building of  $\hat{\alpha}(\infty)$  ( $\otimes$ ) for various depths  $z$ . Plastic yield surface varies from (0) to  $(\infty)$  with the distance between the impact point and studied point.

For a non-void intersection which does not include the initial state, any point of the over-lined segment of the axis  $\hat{\alpha}_{xx} = \hat{\alpha}_{yy} = -\frac{1}{2}\hat{\alpha}_{zz}$  could be available (Fig. 4.b). We choose the closest point to the initial state. When the initial state is included in the non-void intersection (Fig. 4. c), we keep it.

3.3. Influence of the parameters

This model allowed us to investigate the influence of various parameters at a very low cost. One can see in the following Figs. 5 to 8 the influence of depth, shot-speed,

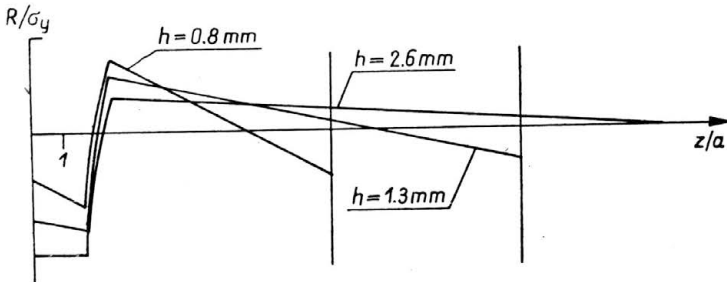


FIG. 5. Influence of thickness of the plate on residual stresses. ( $\sigma_y$ , yield limit,  $a$  radius of contact). Shot-peening conditions  $\sigma_y/E = 2.5 \cdot 10^{-3}$ ,  $C/E = 2 \cdot 10^{-3}$ ,  $V_0 = 40$  m/s,  $r = 0.5$  mm.

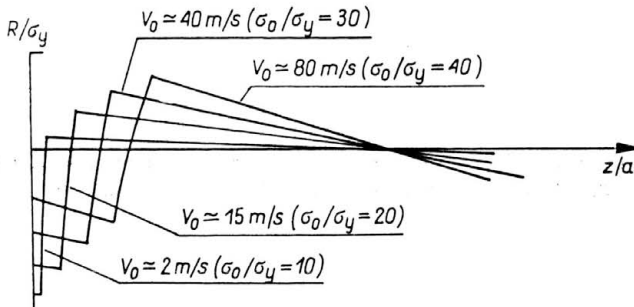


FIG. 6. Influence of the shot speed ( $h = Cste$ ) on residual stresses. ( $\sigma_y$ , yield limit,  $a$  radius of contact).  $\sigma_y/E = 2.5 \cdot 10^{-3}$ ,  $C/E = 2 \cdot 10^{-3}$ ,  $h = 1.3$  mm,  $r = 0.5$  mm.

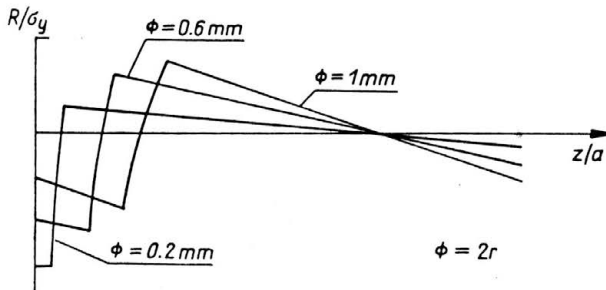


FIG. 7. Influence of the diameter of the bullets on residual stresses.  $\sigma_y/E = 2.5 \cdot 10^{-3}$ ,  $C/E = 2 \cdot 10^{-3}$ ,  $h = 1.3$  mm,  $V_0 = 40$  m/s.

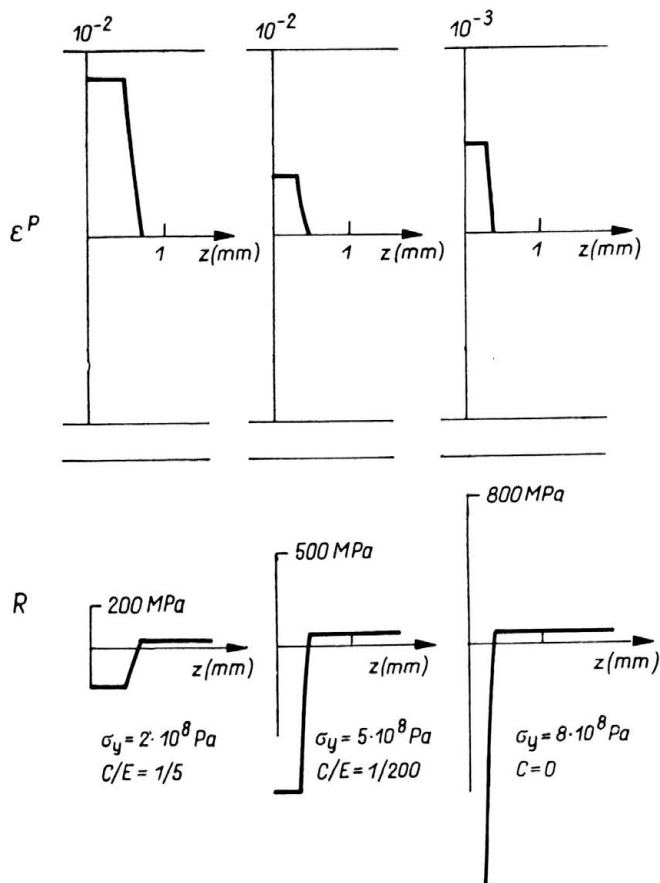


FIG. 8. Influence of the material behaviour  $v_0 = 50$  m/s,  $r = 0.55$  mm,  $h = 20$  mm,  $E = 2 \cdot 10^{11}$  Pa. Simulation of aluminium, standard steel, high limits steel.

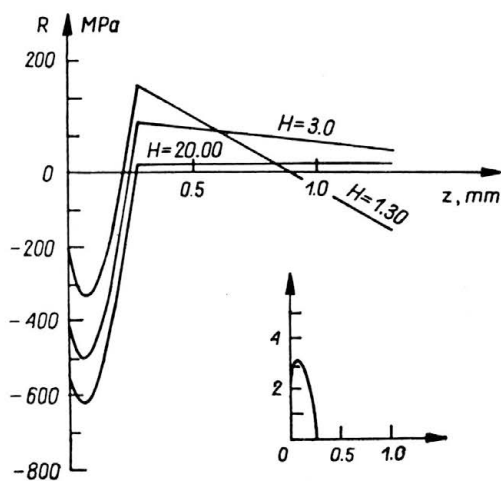


FIG. 9. Experimental results for various thicknesses. (a. Nuku Lari).

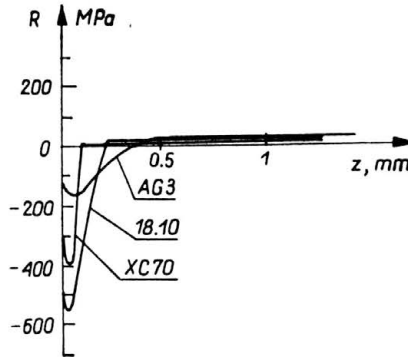


FIG. 10. Experimental results for various materials.

bullet diameter, plastic constants (yield value and hardening modulus) on the residual stresses and deflection, and compare it to the experimental data in Figs. 9 and 10, and experimental values of Almen intensity (deflection of a normalised sample) against speed, depth and bullet diameter in Table 1.

Table 1. Table of deflection

IMAGE OF ALMEN INTENSITY		$\Delta x = 15.875 \text{ mm}$
1. SPEED	$V_0 \text{ (m/s)}$	$f \text{ (mm)}$
	~ 80	0.282
	~ 40	0.197
	~ 15	0.111
	~ 2	0.036
2. WIDTH	$h \text{ (mm)}$	$f \text{ (mm)}$
	0.8	0.047
	1.3	0.197
	2.6	0.053
	5.0	0.015
3. BULLET DIAMETER	$\phi \text{ (mm)}$	$f \text{ (mm)}$
	2	0.343
	1.6	0.296
	1	0.197
	0.2	0.079

All the experimentally observed effects are found with reasonable accuracy. *Very few numerical computations* are needed when a classical numerical computation would have been nearly impossible. So, it appears to be a very suitable tool for industrial purposes.

#### 4. The rolling problem

A similar study was carried out for the rolling problem. In that case, it is difficult to compare with experimental results and very few numerical studies are available.

To demonstrate the efficiency of our direct method, we needed another method to obtain the solution. For this purpose, we chose to apply an original steady-state algorithm based upon some work of Nguyen Quoc Son that we present first.

**4.1. Common basic hypothesis**

We consider a semi-infinite half-space, or infinite plate of depth  $h$  (denoted  $\Omega$ ). The  $\Omega$  domain is made of an elastic-plastic material with linear kinematic strain-hardening.

Over it, an infinite cylinder of radius  $r$  (denoted  $\Omega$ ) is rolling with a constant speed  $V$ . Successive rollings of  $(C)$  on  $(\Omega)$  occur. Under the moving cylinder, we assume the normal stress distribution of Hertz represented by  $p(x)$  on the contact area  $(-a \leq x \leq a)$  in both cases.

It is obvious that a plane strain analysis must be used.

**4.2. Steady state approach**

**4.2.1. Particular hypothesis.** Our purpose is to calculate successive amounts of plastic strain in  $(\Omega)$  for several successive rollings of  $(C)$ ; this approach may concern elastic or plastic shakedown, or ratchetting. The initial state of  $\Omega$  is the natural one. The reference coordinates are linked to the moving cylinder (or the moving load). It follows that the plastic strain rate will only be time-dependent through  $x$  and could be written as

$$(4.1) \quad \dot{\epsilon}^p(x, t) = -V \frac{\partial \epsilon^p}{\partial x}.$$

**4.2.2. Steady state algorithm.** We assume the initial conditions for one rolling as a strain field  $\epsilon_0^p$  which is only a function of the depth;  $\sigma_0$  will be the associated stress field. The

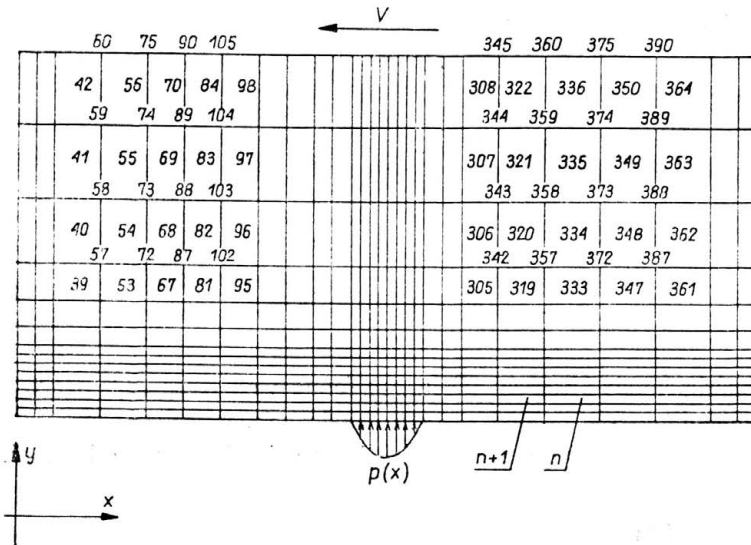


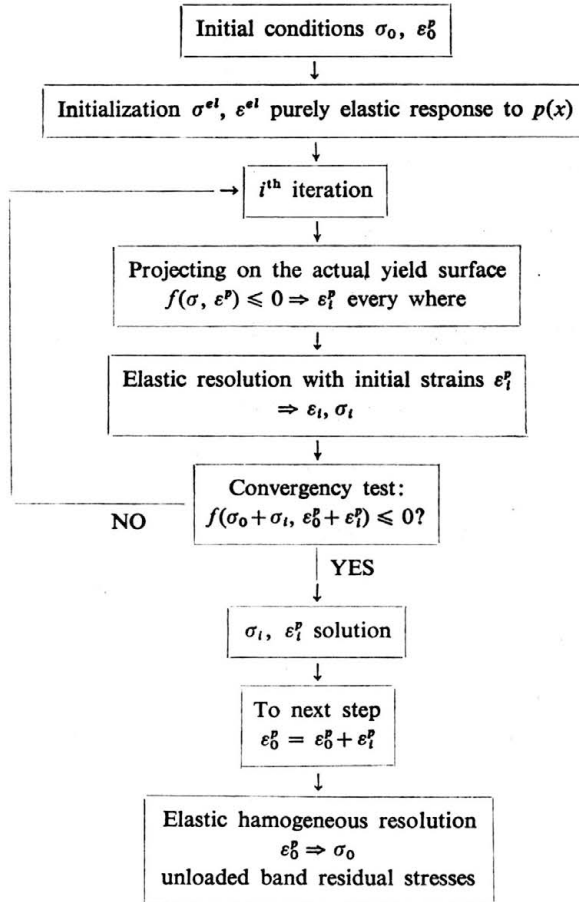
FIG. 11. Mesh and loading conditions for each finite element in the  $x$  direction, the rate of plastic strain

$$\text{is given by } \frac{d\epsilon^p}{dt}(x, t) = -V \frac{\partial \epsilon^p}{\partial x}.$$

elastoplastic solution  $\epsilon^p, \sigma$  in the neighbourhood of the load  $p(x)$  is obtained by a finite element method, using an implicit algorithm (Tabl. 2).

The state of plastic strains and stresses far behind the load and far enough from the boundary appears to be homogeneous with depth and will give the initial conditions for a further rolling (Figs. 11 and 12).

Table 2. Steady state implicit algorithm



4.2.3. Calculating the plastic strain increase in the rolling direction. The main difficulty of the calculus is to give a good evaluation of the space strain rate in the rolling direction. It is obviously linked to the mesh which must be made of strips parallel to the rolling direction. Let us number  $n$  and  $(n + 1)$  two connected elements in the same strips as defined in Figs. 11 and 12.

For a strip of a given depth let  $\epsilon_{i-1}(n + 1)$  be the total strain in the  $(n + 1)^{th}$  element at the  $(i - 1)^{th}$  iteration. We note  $L$  the elasticity operator and calculate

$$(4.2) \quad \sigma' = L(\epsilon_{i-1}(n + 1) - \epsilon_i^p(n)) + \sigma_0.$$

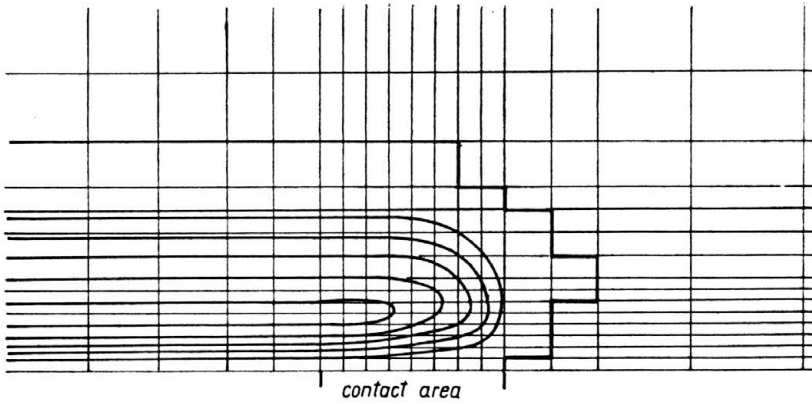


FIG. 12. Isoplastic strain curves after the first step for  $\sigma_0 = 3.8 \sigma_y$ .

Using the von Mises yield criterion, we test

$$(4.3) \quad f(\sigma', \varepsilon_i^p(n) + \varepsilon_0^p) \leq 0?$$

If this inequality is true, the  $(n + 1)^{th}$  element is in the elastic range or elastic unloading. Then

$$(4.4) \quad \varepsilon_i^p(n + 1) = \varepsilon_i^p(n).$$

If the inequality (4.3) is not verified, the  $(n + 1)^{th}$  element is in the plastic range (for loading or unloading). Then the increase of plastic strain  $\varepsilon(n + 1) - \varepsilon(n)$  is evaluated by projection on the actual convex yield surface:

$$(4.5) \quad d\varepsilon_i^p = \varepsilon_i^p(n + 1) - \varepsilon_i^p(n) = d\lambda \frac{\partial f}{\partial \sigma} (\sigma' - d\varepsilon_i^p).$$

**4.2.4. Main results.** This algorithm is purely implicit; hence convergency is ensured whatever the choice of the positive hardening rule, [7]. For the first step, Figs. 11 and 12 give the isoplastic strain curves. In Fig. 13, the same isoplastic strain curves are plotted

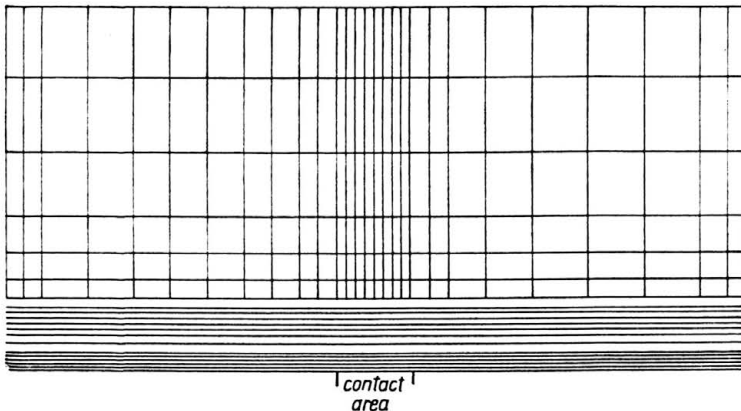


FIG. 13. Isoplastic strain curves after the 10<sup>th</sup> step  $\sigma_0 = 3.8 \sigma_y$ . Elastic shakedown occurred.

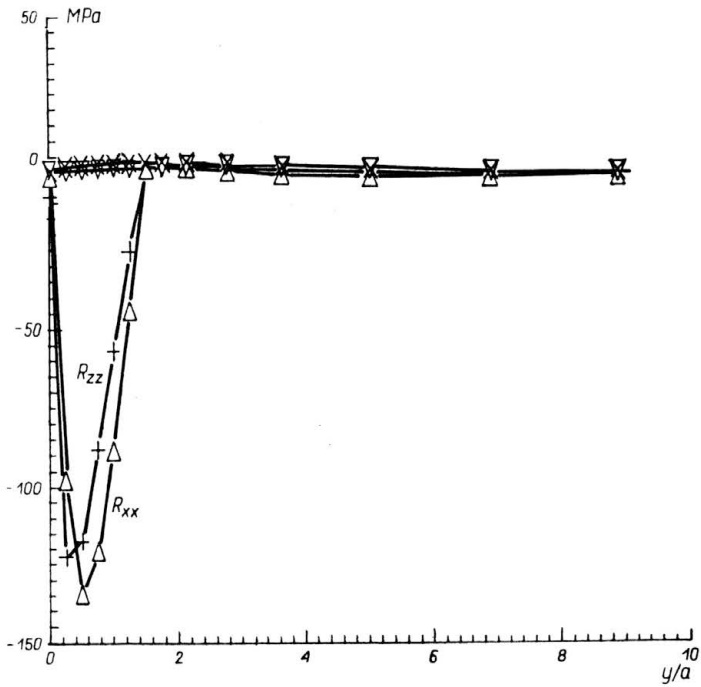


FIG. 14. Distribution of residual stresses with depth.  $\sigma_y = 200$  MPa,  $\sigma_0 = 3.8 \sigma_y$ .

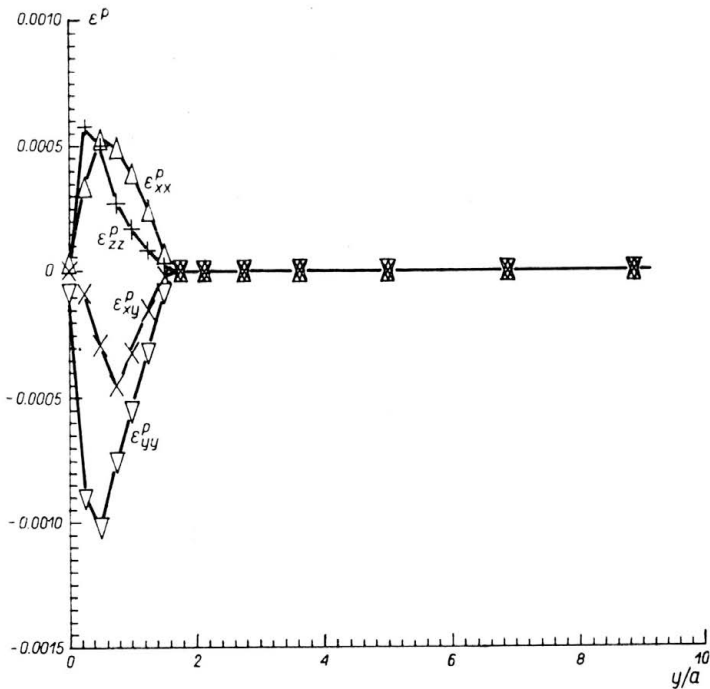


FIG. 15. Distribution of plastic strain with depth.  $\sigma_0 = 3.8 \sigma_y$ ,  $\sigma_y = 8000$  MPa,  $E = 200.000$  MPa.

for the tenth step when elastic shakedown is practically achieved. The residual stresses and plastic strain distribution with depth are plotted in Figs. 14 and 15 for this tenth step in the elastic range.

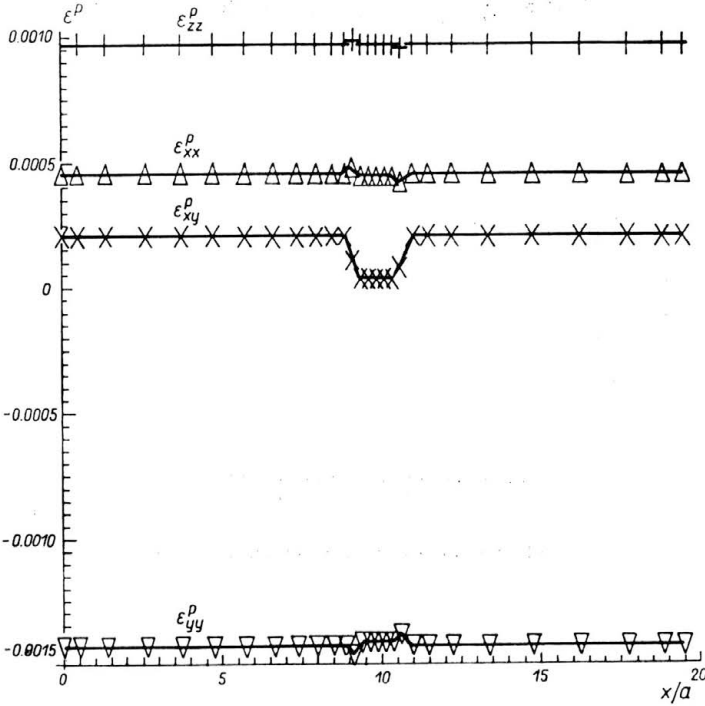


FIG. 16. Distribution of plastic strains in the strip at depth  $z = 3a/8$ .

For larger  $\sigma_0$  stresses plastic shakedown will be observed as could be clearly seen in the plastic strain distribution in a strip (Fig. 16). A periodic increase of plastic strain just under the load is observed.

**4.3. Straightforward method**

Basic hypothesis and application of this method are quite similar to Sect. 2. The choice of the transformed variable  $\hat{\alpha}$ , which depends only on the depth  $z$ , is a little more complicated than previously and varies according to whether elastic or plastic shakedown is obtained. The elastic loading is given by the Hertz theory for the contact of an infinite cylinder on a semi-infinite half-space with a plane boundary.

Figure 17 shows the results of the direct method compared with the previous ones (Sect. 3.2). Both results have been obtained with the same linear kinematic hardening behaviour and loading path.

Considering the arbitrary choice of the transformed variables and, on the other hand, the use of a rather coarse finite element mesh, compared with the "exact" solution of

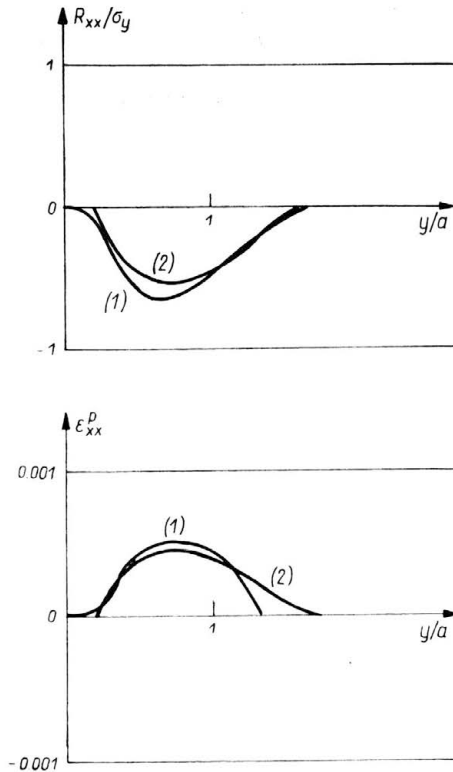


FIG. 17. Comparison between both methods for residual stresses and plastic strain under the loading ( $\sigma_0 = 3.8 \sigma_y$ ).

1 — results obtained by steady state algorithm. 2 — results obtained by straightforward approach.

the Hertz problem, we have a very good agreement between the results of these two methods.

The advantage of the straightforward direct method is essentially the *very quick and cheap answer*. Further studies for *other hardening laws* could *only be* developed using the steady-state approach.

## References

1. J. ZARKA, J. CASIER, *Elastic plastic response of a structure to cyclic loading: practical rules*, Mechanics Today, Vol. 6, Ed. NEMAT-NASSER, Pergamon Press, 1979.
2. J. ZARKA, G. INGLEBERT, *Sur une nouvelle analyse simple des structures inélastiques*, Cours à l'Université de la Calabre, Cosenza, Italie 1980.
3. J. ZARKA, G. INGLEBERT, *Structural analysis including kinematical hardening and creep*, L/11/3, 6th SMIRT, Paris, Août 1981.
4. G. INGLEBERT, *Analyse simplifiée des structures élastoviscoplastiques sous chargements cycliques*, Thèse, Paris VI, 17 Janvier 1984.
5. B. HALPHEN, Q. S. NGUYEN, *Sur les matériaux standards généralisés*, J. de Mécanique, **14**, 1, 39-63, 1975.

6. J. ZARKA, J. FRELAT, *Détermination des contraintes résiduelles et des déformations lors des roulements successifs d'un corps cylindrique sur un massif semi-infini élastoplastique*, C.R.Acad. Sci., **292**, 4, Paris, 6 Avril 1981.
7. Q. S. NGUYEN, *On the elastic plastic initial boundary value problem and its numerical integration*, Int. J. for Numerical Methods in Eng., **11**, 817-832, 1977.

LABORATOIRE DE MECANIQUE DES SOLIDES  
ECOLE POLYTECHNIQUE, PALAISEAU, FRANCE.

*Received October 29, 1984.*

---